RNA (1997), 3:476–488. Cambridge University Press. Printed in the USA.

Variable regions V13 and V3 of *Saccharomyces cerevisiae* contain structural features essential for normal biogenesis and stability of 5.8S and 25S rRNA

RIENK E. JEENINGA, YVON VAN DELFT, MURIEL DE GRAAFF-VINCENT, ANITA DIRKS-MULDER, JAAP VENEMA, and HENDRIK A. RAUÉ

Department of Biochemistry & Molecular Biology, IMBW, BioCentrum Amsterdam, Vrije Universiteit De Boelelaan 1083, 1081 HV Amsterdam, The Netherlands

ABSTRACT

The homologous ribosomal RNA species of all organisms can be folded into a common "core" secondary structure. In addition, eukaryotic rRNAs contain a large number of segments, located at fixed positions, that are highly variable in size and sequence from one organism to another. We have investigated the role of the two largest of these variable regions in *Saccharomyces cerevisiae* 25S rRNA, V13, and V3, by mutational analysis in a yeast strain that can be rendered completely dependent on the synthesis of mutant (pre-)rRNA. We found that approximately half of variable region V13 can be deleted without any phenotypic effect. The remaining portion, however, contains multiple structural features whose disturbance causes serious growth defects or lethality. Accumulation of 25S rRNA is strongly reduced by these mutations, at least in part because they inhibit processing of ITS2. Removal of even a relatively small portion of V3 also strongly reduces the cellular growth rate and larger deletions are lethal. Interestingly, some of the deletions in V3 cause accumulation of $27S_A$ pre-rRNA and, moreover, appear to interfere with the close coupling between the processing cleavages at sites A3 and $B1_S$. These results demonstrate that both variable regions play an important role in 60S subunit formation.

Keywords: expansion segments; ribosomal RNA; rRNA processing; yeast

INTRODUCTION

Sequence comparison between the rRNAs of different organisms shows a patchwork of conserved and non-conserved sequences. Nevertheless, large portions of each of the rRNA species can be folded into a highly conserved secondary structure even in the regions showing little sequence similarity (Gutell et al., 1993; De Rijk et al., 1996; Schnare et al., 1996; Van der Peer et al., 1996). As has become evident from numerous studies, this "universal core" rRNA structure, of which the *Escherichia coli* rRNA species can be considered as the paradigm, plays a pivotal role in the various steps of protein translation (reviewed in Noller, 1991; Noller et al., 1992, 1995; O'Connor et al., 1995; Triman, 1996a, 1996b).

In eukaryotes, however, there are numerous regions, distributed at fixed positions along the rRNA core, that differ to a large extent in both primary and secondary structure between different organisms and even between different genes of the same organism (reviewed in Gerbi, 1996). These variable regions or expansion segments account for most of the size differences between pro- and eukaryotic rRNAs. At present, the function of these regions is unclear. From data obtained by in vivo mutagenesis, it appears that structural alteration of some variable regions remains without any phenotypic effect. Mutations in others, however, influence the formation and/or the function of ribosomes. Analysis of *Saccharomyces cerevisiae* 25S rRNA showed that it was possible to introduce 18 nt into variable region V2 [cf. Fig. 1; the nomenclature of Raué et al. (1988) is used] without any detectable effect in vivo (Musters et al., 1989b; Venema et al., 1995a). Removal of variable region V9 of *S. cerevisiae* 25S rRNA or replacing it by its mouse or *Tetrahymena thermophila* counterpart did not interfere with ribosome biogenesis

Reprint requests to: H.A. Raué, Department of Biochemistry & Molecular Biology, IMBW, BioCentrum Amsterdam, Vrije Universiteit, De Boelelaan 1083, 1081 HV Amsterdam, The Netherlands; e-mail: raue@chem.vu.nl.

Abbreviations: LSU, large subunit; SSU, small subunit; bp, base pair(s); kb, kilobase pair(s); r-protein, ribosomal protein

(Musters et al., 1991), although yeast cells completely dependent on such mutant 25S rRNA showed a reduced growth rate, indicating that removal of V9 causes a functional defect (Kooi, 1995). In *T. thermophila*, it was possible to insert 119 nt into variable regions V3 or V18 of the LSU rRNA without any deleterious effect on cell growth (Sweeney & Yao, 1989). On the other hand, insertions of 119 nt or 2,300 nt into the V13 region of the *T. thermophila* LSU rRNA were lethal (Sweeney & Yao, 1989). Further analysis of V13 in *T. thermophila* demonstrated that it could be replaced by the corresponding region from various other organisms, including yeast, but not by a totally unrelated sequence (Sweeney et al., 1994). This observation provided the first evidence that a variable region possesses an evolutionarily conserved function. Because sequence similarity between the V13 region of *T. thermophila* and its counterparts from other organisms is very limited, the functional equivalence is likely to originate from common secondary (Schnare et al., 1996) or higher-order structure. The results obtained upon mutational analysis of different variable regions in the SSU rRNA revealed a similar variety of effects (Musters et al., 1989b; Sweeney et al., 1993; Van Nues et al., 1997).

In this paper, we present a study on the role of the yeast 25S rRNA variable regions V13 and V3 by in vivo deletion analysis using the "in vivo Pol II" system (Venema et al., 1995a), which allows yeast cells to be made completely dependent on synthesis of mutant, plasmid-encoded rRNA. The results demonstrate that both variable regions contain distinct structural elements that are important or even essential for ribosome biogenesis, in particular, the formation and accumulation of 25S rRNA.

RESULTS

Experimental design

The majority of previous studies addressing the functional importance of variable regions in rRNA have used insertion mutagenesis (Musters et al., 1989a; Sweeney & Yao, 1989; Sweeney et al., 1993; Venema et al., 1995a). This carries the hazard that the resulting functional defect is due to disturbance of the higher-order structure of the core by the inserted sequence rather than the destruction of a functional element within the variable region (Gerbi, 1996; Van Nues et al., 1997). Therefore, we decided to analyze the functional importance of the variable regions V13 and V3 of 25S rRNA by deletion analysis. The size and location of the deletions were based on the secondary structure models for V13 and V3 derived by comparative structural analysis (Gutell et al., 1993; Schnare et al., 1996) and designed such that they deleted (combinations of) individual secondary structure elements. The proposed secondary structures of the two variable regions and the putative secondary structures of the various mutant forms are depicted in Figure 1. Each of the deletions was tested in the in vivo Pol II system (Venema et al., 1995a). This system employs a special yeast strain, YJV100, which lacks RNA polymerase I due to a disruption of the gene encoding the second-largest subunit of this enzyme (Nogi et al., 1991). The strain is rescued by the presence of multiple integrated copies of a wild-type rDNA unit under control of the glucose-repressible *GAL7* promoter, which is recognized by RNA polymerase II. Mutations in the rDNA were analyzed by introducing them into YJV100 on the episomal plasmid pJV12 (2μ- *URA3*) as part of an rDNA unit under control of the constitutive *PGK1* promoter. Upon a change in carbon source from galactose to glucose, transcription of the wild-type *GAL7*-driven rDNA units is shut down and the YJV100 transformants become completely dependent upon the plasmid-derived, mutant rRNA. The presence of small, neutral oligonucleotide tags in both the 18S (Beltrame et al., 1994) and 25S rRNA (Musters et al., 1989b) genes of pJV12 allows the specific detection of plasmid-derived, mature rRNA molecules and their precursors even in the presence of the wild-type species.

Mutations in V13 and V3 affect cell growth

The effect of the various mutations in the V13 and V3 variable regions was first assessed globally by analyzing the growth of YJV100 transformants on glucose. YJV100 transformants carrying the respective mutant derivatives of pJV12 were first selected for uracil prototrophy on YNB-galactose, followed by screening for their ability to grow on both solid and liquid glucose-based medium at 30 °C. The results (Fig. 2) show that removal of the left arm E20_1 [helix numbering according to De Rijk et al. (1996)] of the Y-shaped variable region V13 (mutant V13Δ97) had no effect on the growth rate (Fig. 2A). When the deletion was extended to include helix E20_2 (mutant V13Δ111), the doubling time increased more than twofold (Fig. 2B). This growth defect could be overcome by reconstruction of the E20_2 helix with a completely different primary sequence (mutant V13Δ97C; Fig. 2C). Almost complete removal of the V13 region (mutant V13Δ131; Fig. 2D) was lethal, in accordance with the results of Sweeney et al. (1994) for *Tetrahymena*. These experiments clearly demonstrate that about half of V13 (i.e., helix E20_1) is completely dispensable. Of the remaining portion, only helix E20 contains essential structural elements, whereas the secondary, but not the primary, structure of E20_2 is important for normal cellular growth. All transformants were also tested for growth on YNB-glucose plates at 15°, 23°, and 37 °C. No temperature-dependent effects on growth were observed (data not shown).

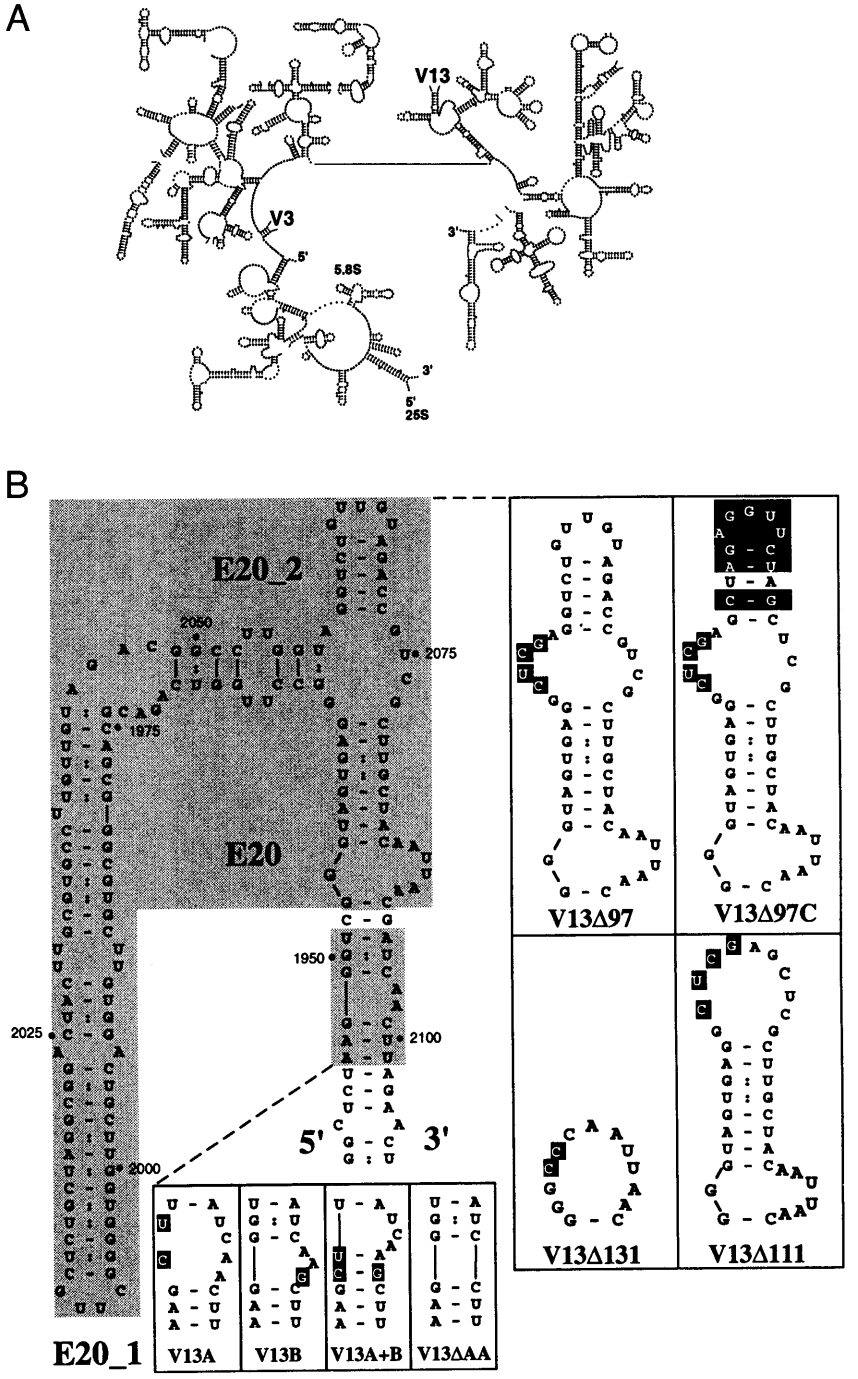

FIGURE 1. Secondary structure models for variable regions V13 and V3 of *S. cerevisiae* 25S rRNA. **A:** Location of the V13 and V3 variable regions relative to the conserved "core" of the LSU rRNA. **B:** Secondary structure model of V13. **C:** Secondary structure model of V3 (Schnare et al., 1996). Regions in which the mutations were made are shaded. Putative secondary structures of these regions in the different V13 and V3 mutants are shown in the boxes. Nucleotides differing from the wild-type sequence are in reversed contrast. Helix numbering is according to De Rijk et al. (1996). The arrow in C indicates the position corresponding to the site of a neutral insertion into *T. thermophila* 26S rRNA (Sweeney et al., 1996). (*Figure continues on facing page.*)

To identify possible functional elements in the lower portion of the E20 helix, we mutagenized the region containing the two highly conserved (Schnare et al., 1996) bulged A residues. The introduction of two point mutations into the 5′ side (mutant V13A) or the insertion of an extra G into the 3′ side (mutant V13B), each of which creates a *Hin*d III site, did not influence the cellular growth rate (Fig. 2E,F). When these two neutral mutations were combined, however, yielding mutant V13A+B, the YJV100 transformants failed to grow on glucose (Fig. 2G). Removal of the bulged A residues (mutant V13ΔAA) also proved to be lethal (Fig. 2H).

Analysis of a set of progressively larger deletion mutations in variable region V3 (cf. Fig. 1) demonstrated that removal of 44 nt comprising the outermost portion of the C1_2 helix (mutant V3Δ44) caused about twofold reduction in growth rate (Fig. 2I), whereas deletion of the complete C1_2 stem-loop structure (mutant V3Δ93) resulted in a lethal phenotype (Fig. 2J). An even larger deletion (mutant V3Δ181), which reduces V3 to the approximate size of its bacterial counterpart, was found to be lethal as well. Again there were no temperature-dependent effects of any of these mutations on growth (data not shown).

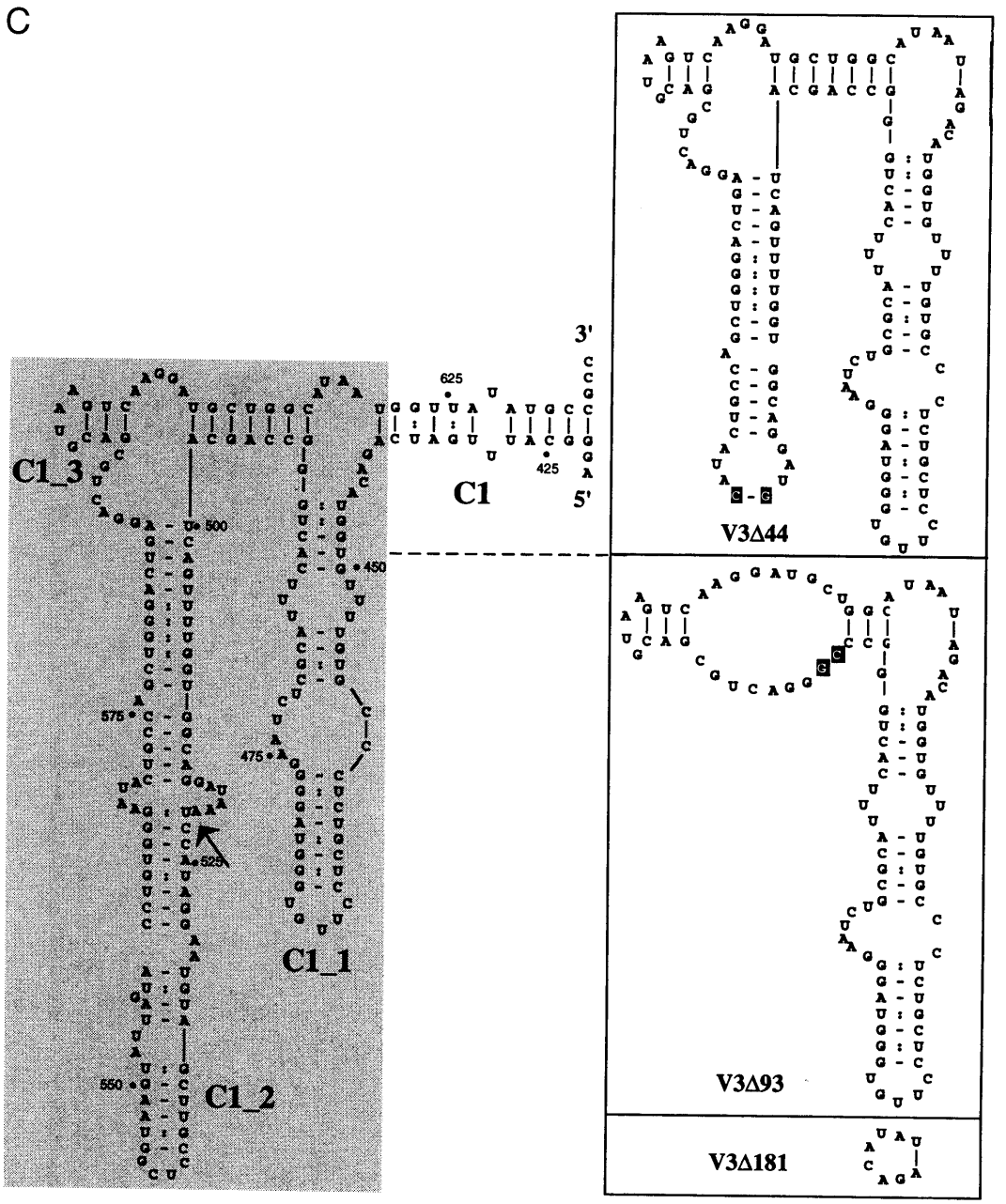

FIGURE 1. *Continued.*

Mutations in V13 and V3 reduce the level of 25S rRNA

To determine whether the negative effect of V13 and V3 mutations on cell growth is due to inhibition of ribosome biogenesis or the formation of functionally defective ribosomes, we assayed the levels of the mature rRNA species in the various YJV100 transformants after growth on glucose. Total RNA was isolated from YJV100 transformants 16 h after a shift from galactose- to glucose-based medium and analyzed by northern hybridization using oligonucleotides complementary to the tags in 18S and 25S rRNA (cf. Fig. 4A). Hybridization signals were quantified using a phosphorimager. In the different V13 mutants that grew with a wild-type doubling time (i.e., mutants V13A, V13B, V13Δ97, and V13Δ97C), the ratio of 18S to 25S rRNA was the same as in the wild-type control (data not shown). In the slow-growing V13Δ111 mutant, the level of 25S rRNA was reduced by about 30% relative to the control (Fig. 3A, cf. lanes 5 and 6 to lane 2), and, in the nonviable mutants V13ΔAA, V13Δ131, and V13A+B, only very small amounts of 25S rRNA were detectable (Fig. 3A, cf. lanes 3 and 4, 7 and 8, 9 and 10 to lane 2)

Similar results were obtained for the V3 mutants. The lethal mutations V3Δ181 and V3Δ93 reduced 25S rRNA to a level below the detection limit (Fig. 3B, cf. lane 3 and 5 to lane 2), whereas the V3Δ44 mutation

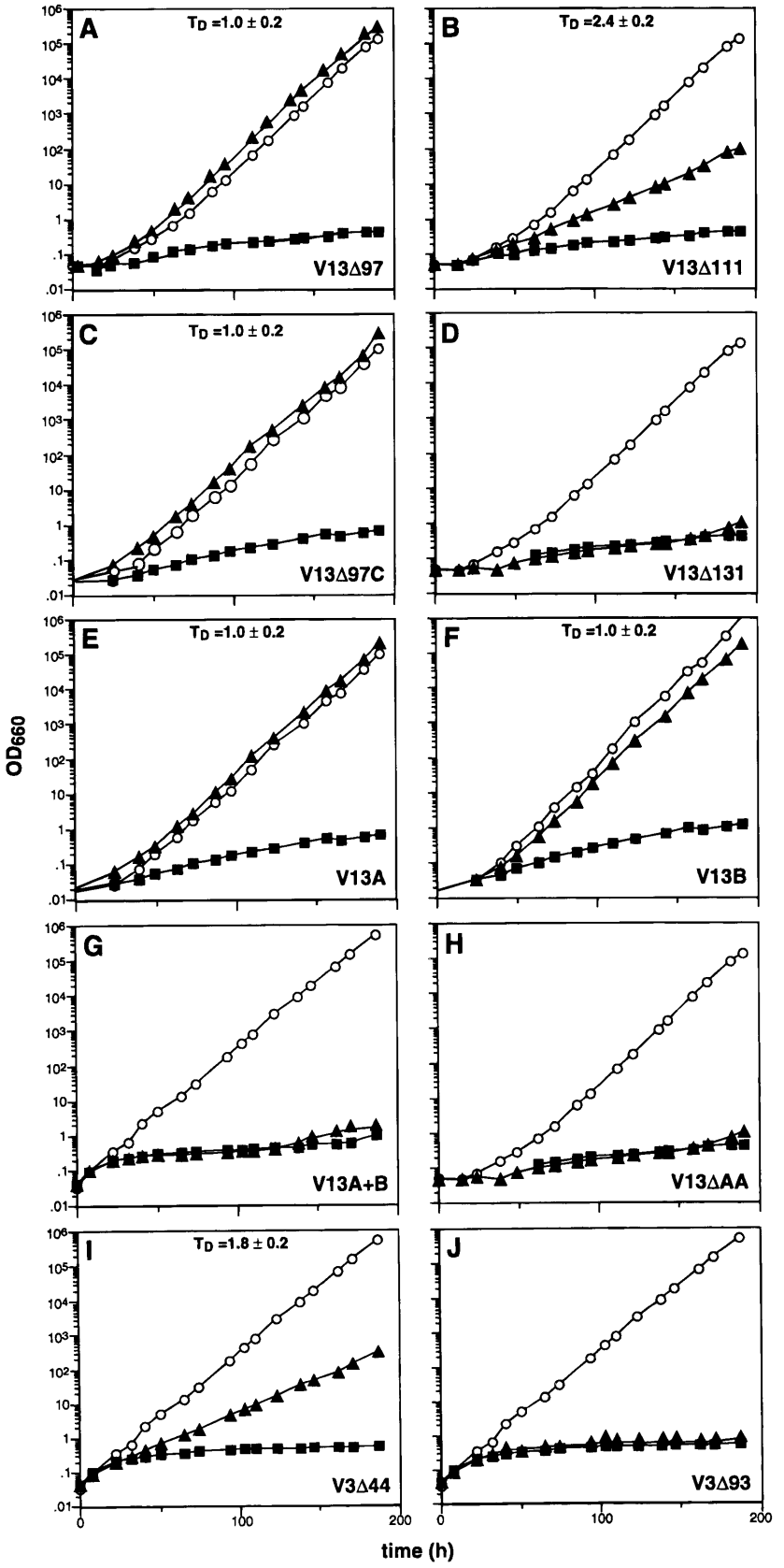

FIGURE 2. Effect of the various V13 and V3 mutations on cell growth. YJV100 transformants carrying the respective pJV12 derivatives were transferred from galactose-based to glucose-based medium and growth was followed by measuring the OD_{660} at regular intervals (▲). If necessary, cultures were diluted to maintain exponential growth. Transformants carrying the wild-type pJV12 (○) or the "empty" vector (■) were analyzed in parallel. **A–H:** V13 mutants. **I–J:** V3 mutants. Relative growth rates (T_D) were determined by dividing the doubling time of the mutant by the doubling time of the wild-type control. For each mutation, the average value calculated from testing at least four different transformants is given and the standard deviation is indicated.

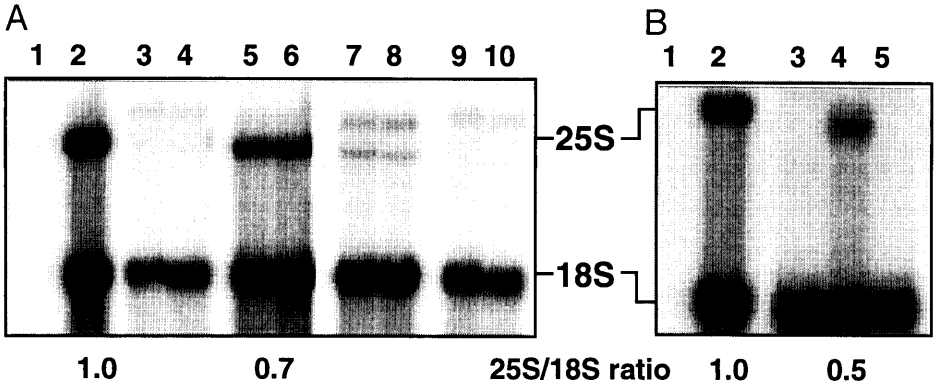

FIGURE 3. Northern analysis of 18S and 25S rRNA levels in V13 and V3 mutants. Total RNA was extracted from YJV100 transformants grown for 16 h on YNB-glucose and analyzed by northern hybridization using the oligonucleotides complementary to the tags in 18S and 25S rRNA as probes. **A:** Analysis of V13 mutants exhibiting growth defects. Lane 1, YJV100 carrying a plasmid without a tagged rDNA unit; lane 2, YJV100 carrying the wild-type pJV12 plasmid; lanes 3 and 4, mutant V13ΔAA; lanes 5 and 6, mutant V13Δ111; lanes 7 and 8, mutant V13Δ131; lanes 9 and 10, mutant V13A+B. **B:** Analysis of V3 mutants. Lane 1, YJV100 carrying a plasmid without a tagged rDNA unit; lane 2, YJV100 carrying the wild-type pJV12 plasmid; lane 3, mutant V3Δ181; lane 4, mutant V3Δ44; lane 5, mutant V3Δ93. Positions of the mature 18S rRNA and 25S rRNA are indicated. For mutants V13Δ111 and V3Δ44, the 25S/18S ratio relative to that of the wild-type control is indicated. The value is the average of five independent assays. Note that the specific activity of the 18S and 25S probes was different, which accounts for the signal of the latter being less intense than that of the former.

resulted in a twofold reduction of the mature 25S rRNA level (Fig. 3B, cf. lane 4 to lane 2), in accordance with its intermediate growth phenotype.

These results demonstrate that the amount of 25S rRNA present in the various mutants correlates well with their respective growth phenotype, indicating that the observed growth deficiencies are primarily due to defects in the synthesis and/or stability of the 25S rRNA.

Mutations in V13 and V3 inhibit pre-rRNA processing

The effect of the V13 and V3 mutations on pre-rRNA processing was analyzed by northern hybridization using a set of oligonucleotides complementary to the transcribed spacer regions (cf. Fig. 4A). Because pre-rRNA processing is essentially complete within 10 min, and the background transcription of chromosomal *GAL7*-driven wild-type rDNA units is negligible (Venema et al., 1995a; Van Nues et al., 1997), all precursors detected in glucose-grown YJV100 transformants will be derived from the plasmid-borne mutant rDNA units. The pre-rRNA processing pathway in yeast is outlined in Figure 4B. Probe 1A detects the 20S pre-rRNA, which was used as the internal standard because its level is unlikely to be affected by any of the mutations in V13 or V3 (Van Nues et al., 1993, 1995). The $27S_A$ pre-rRNA was assayed using probe 1D, which recognizes both the $27S_{A2}$ and $27S_{A3}$ species. Probe 2A simultaneously detects the $27S_A$ and $27S_B$ pre-rRNAs. It is important to note that, under normal conditions, the hybridization signal predominantly reflects the level of the latter species, which is about 10 times more abundant than the $27S_A$ precursor. Total RNA was again isolated from the various YJV100 transformants 16 h after transfer from galactose- to glucose-based medium. Typical experiments are shown in Figure 5A (V13 mutants) and B (V3 mutants), whereas in Figure 5C and D, the data from a number of independent experiments for the two sets of mutations have been compiled. Pre-rRNA levels are given relative to the levels observed in YJV100 control cells carrying pJV12.

V13 mutants

In YJV100 transformants carrying V13 mutations that did not affect cell growth (i.e., V13A, V13B, V13Δ97, and V13Δ97C), the levels of the $27S_A$ and $27S_{A+B}$ pre-rRNAs were indistinguishable from those in pJV12 control transformants (data not shown). The V13 mutants showing a growth defect also contain wild-type levels of $27S_A$ pre-rRNA (Fig. 5A,C). However, in the slow-growing V13Δ111 mutant, $27S_{A+B}$ pre-rRNA was slightly elevated (Fig. 5A, lanes 5 and 6; Fig. 5C), whereas the lethal V13ΔAA, V13Δ131, and V13A+B mutations increased the level of the $27S_{A+B}$ precursors approximately threefold (Fig. 5B, lanes 3 and 4, lanes 7 and 8, lanes 9 and 10, respectively; Fig. 5C). Thus, we conclude that these mutations delay ITS2 processing, leading to an increase in $27S_B$ pre-rRNA.

The same mutations were also cloned into pJV16, which contains an additional oligonucleotide tag in the 5.8S rRNA sequence (Henry et al., 1994). Northern analysis of total RNA isolated 16 h after shifting the YJV100 transformants to glucose-based medium, using the oligonucleotide complementary to this tag, showed a good correlation between the levels of 5.8S and 25S

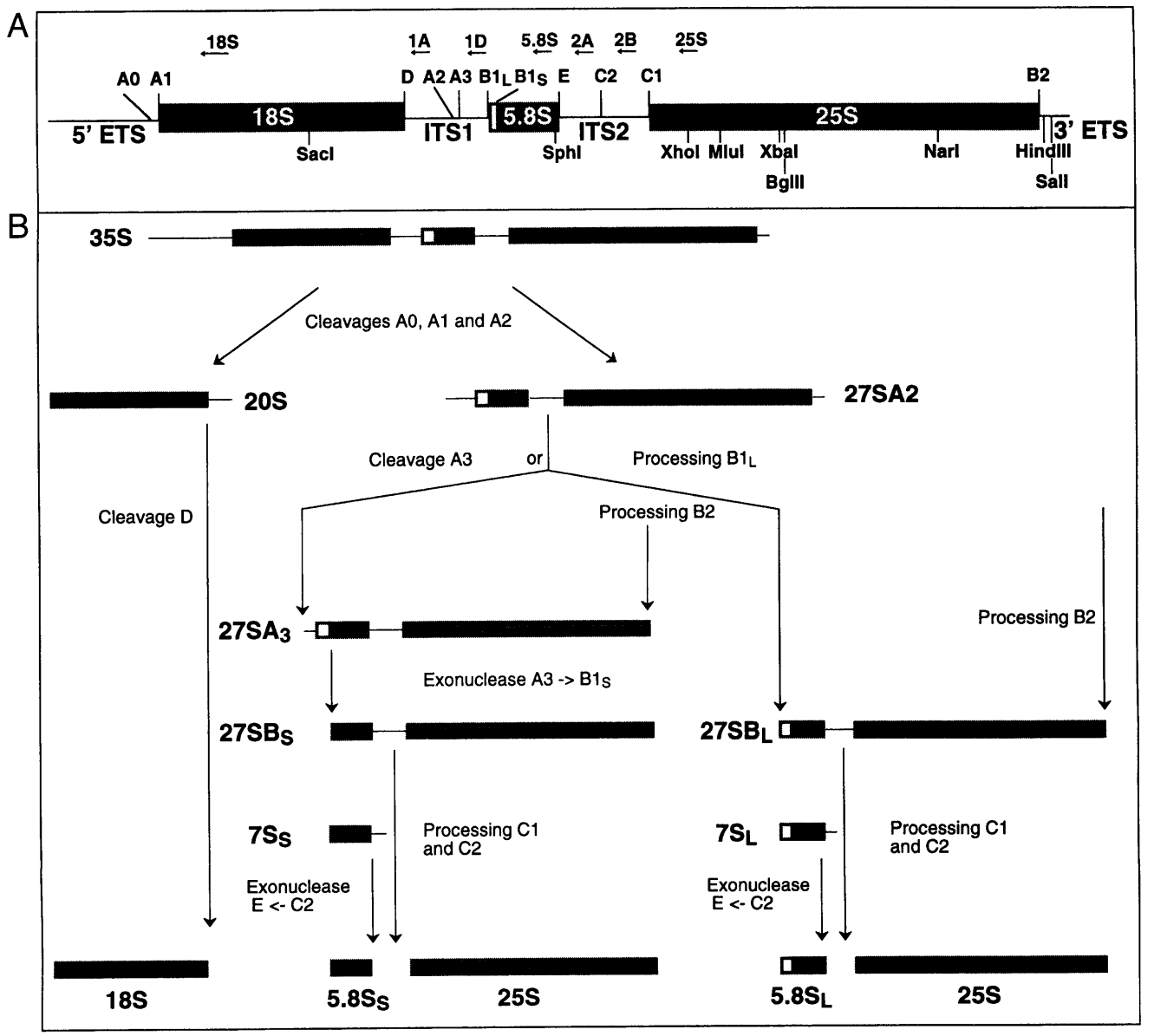

FIGURE 4. Pre-rRNA processing in *S. cerevisiae*. **A:** Schematic representation of the yeast rDNA unit. Regions encoding the mature rRNAs and transcribed spacers are indicated by shaded bars and thin lines, respectively. Locations of the different processing sites are shown. Positions of the probes used in this study are indicated by arrows. Restriction sites used to make subclones are indicated. **B:** Pre-rRNA processing pathway (see Raué & Planta, 1995; Venema & Tollervey, 1995 for recent reviews).

rRNA in all mutants (cf. Figs. 3, 6A). Compared to control cells, the level of 5.8S rRNA in the V13Δ111 mutant was roughly the same as in the wild-type control (Fig. 6A, lane 3), whereas tagged 5.8S rRNA was (virtually) absent in the V13Δ131, V13ΔAA, and V13A+B mutants (Fig. 6A, lanes 4–6). However, using probe 2A, we could detect both $7S_S$ and $7S_L$ pre-rRNA, the immediate precursor of 5.8S rRNA, in the latter set of mutants (Fig. 6B, lanes 4–6). Primer extension using the oligonucleotide complementary to the 25S tag or probe 2B showed the $B1_L$ and $B1_S$ stops to have increased in concert in case of the V13Δ111, V13Δ131, V13ΔAA, and V13A+B mutants (Fig. 7, lanes 2–6). Processing was found to be correct at the nucleotide level in all cases. The accumulation of $27S_B$ pre-rRNA in these mutants thus reflects an increase in both $27S_{BS}$ and $27S_{BL}$ pre-rRNA. The presence of detectable amounts of 7S rRNA in the V13Δ131, V13ΔAA, and V13A+B mutants indicates that, despite the absence of mature 5.8S and 25S rRNA, at least some processing of $27S_B$ pre-rRNA still occurs. Apparently, any mature rRNA formed in these mutants is degraded rapidly.

V3 mutants

Analysis of the pre-rRNA species in the V3Δ44 mutant showed that both the $27S_A$ and $27S_{A+B}$ pre-rRNAs were present at wild-type levels (Fig. 5B, lane 4; Fig. 5D).

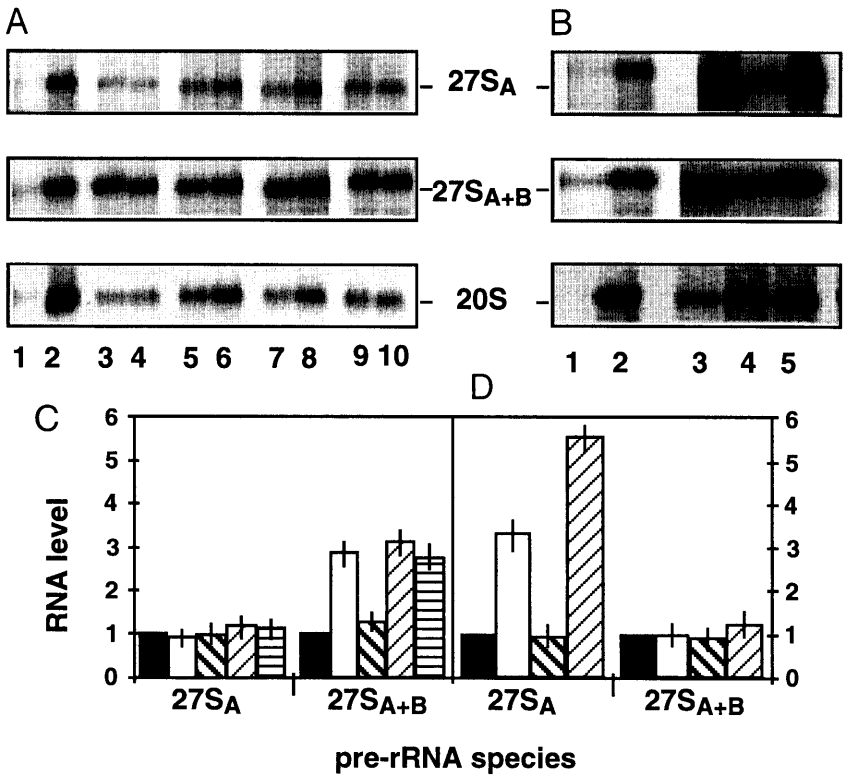

FIGURE 5. Northern analysis of $27S_A$ and $27S_B$ pre-rRNA in V13 and V3 mutants. Total RNA was extracted from YJV100 transformed with the pJV12 derivatives 16 h after transfer from galactose- to glucose-based medium. RNA was analyzed by northern hybridization. The following probes were used (cf. Fig. 4). Probe 1A specifically recognizes 20S pre-rRNA. Probe 1D detects both $27S_{A2}$ and $27S_{A3}$ pre-rRNA. Probe 2A simultaneously detects all 27S pre-rRNAs (both $27S_A$ and $27S_B$). **A:** V13 mutants. Lane 1, YJV100 cells transformed with an "empty" vector; lane 2, wild-type pJV12; lanes 3 and 4, mutant V13ΔAA; lanes 5 and 6, mutant V13Δ111; lanes 7 and 8, mutant V13Δ131; lanes 9 and 10, mutant V13A+B. **B:** V3 mutants. Lane 1, YJV100 cells transformed with an "empty" vector; lane 2, wild-type pJV12; lane 3, mutant V3Δ181; lane 4, mutant V3Δ44; lane 5, mutant V3Δ93. **C:** Quantification of $27S_A$ and $27S_{A+B}$ levels in the V13 mutants. ■, YJV100 carrying wild-type pJV12. □, Mutant V13ΔAA. ▧, Mutant V13Δ111. ▨, Mutant V13Δ131. ▤, Mutant V13A+B. **D:** Quantification of $27S_A$ and $27S_{A+B}$ levels in the V3 mutants. ■, YJV100 carrying the wild-type pJV12. □, Mutant V3Δ181. ▧, Mutant V3Δ44. ▨, Mutant V3Δ93. Hybridization signals of the pre-rRNAs were quantified relative to the signal obtained with the wild-type control using a phosphorimager. 20S pre-rRNA was used as internal standard. Each value is the average of at least 5 independent transformants. The standard deviation is indicated by error bars.

The reduction in mature 25S rRNA observed in mutant V3Δ44, therefore, is likely to be the result of increased turnover of this rRNA, e.g., due to an assembly defect. In transformants carrying the V3Δ93 and V3Δ181 mutations, the level of the $27S_A$ pre-rRNA was elevated by a factor of 3.5 and 5.5, respectively. However, there was no significant increase in the total amount of $27S_{A+B}$ pre-rRNA detected by the ITS2 probe (Fig. 5B, lanes 3 and 5; Fig. 5D). Thus, the level of the $27S_B$ precursor may in fact be reduced in these mutants. These results suggest that the V3Δ93 and V3Δ181 mutations cause a substantial delay in processing at site B1.

Mutations V3Δ93 and V3Δ181 were also cloned into plasmid pJV16. Northern analysis using the probe hybridizing to the 5.8S rRNA tag failed to detect either $5.8S_S$ or $5.8S_L$ rRNA in total RNA isolated from the respective YJV100 transformants after growth on glucose (Fig. 6C, lanes 3–6). As in the case of the lethal V13 mutations, both $7S_S$ and $7S_L$ pre-rRNA were detectable using probe 2A (Fig. 6D, lanes 3–6), indicating that at least some processing of ITS2 occurs in these mutants.

To analyze the effects of the V3 mutations on processing of the different $27S_A$ and $27S_B$ pre-rRNAs in more detail, we mapped the 5′ ends of these precursors by primer extension using the oligonucleotide complementary to the tag in 25S rRNA. We observed no significant differences in the ratios of the stops corresponding to sites A2, A3, $B1_S$, and $B1_L$ for the mutant V3Δ44 compared to the wild-type control (Fig. 8; cf. lanes 1 and 6 to lane 2). However, in case of the V3Δ93 and V3Δ181 mutants, extension from the same primer showed that, although stops at sites A2, A3, and $B1_L$ were clearly visible, no signal corresponding to $B1_S$ could be detected (Fig. 8A compare lanes 3 and 4 to lanes 1 and 6). When primer extension was performed from within ITS2 using probe 2B, essentially the same qualitative and quantitative pattern of stops was found, except that now, to our surprise, both $B1_L$ and $B1_S$ could be detected in the V3Δ93 as well as in the V3Δ181 mutant (Fig. 8B, lanes 3 and 4). These data clearly suggest that the V3Δ93 and V3Δ181 deletions alter the normal order of events after cleavage at site A3. Ap-

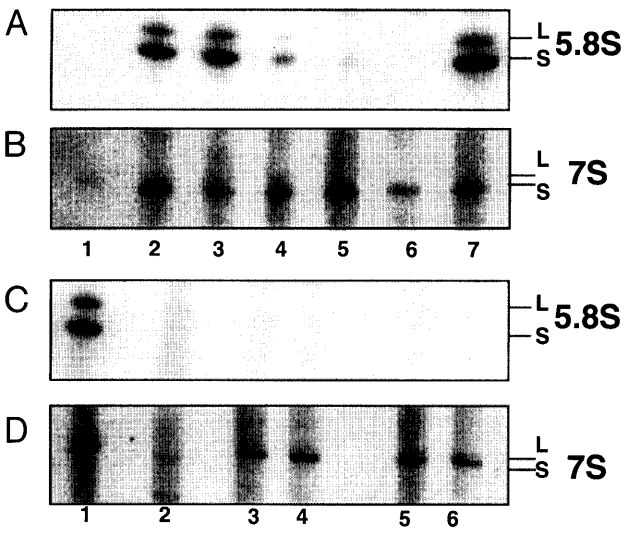

FIGURE 6. Northern analysis of 5.8S and 7S (pre-)rRNA in V13 and V3 mutants. Total RNA was extracted from YJV100 transformed with the pJV16 derivatives carrying the V13 or V3 mutations 16 h after transfer from galactose- to glucose-based medium. RNA was analyzed by northern hybridization using an oligonucleotides complementary to the 5.8S tag (**A,C**) or probe 2A (**B,D**). **A,B:** Lane 1, YJV100 cells carrying a plasmid without an rDNA unit; lane 2, wild-type pJV16; lane 3, mutant V13Δ111; lane 4, mutant V13Δ131; lane 5, mutant V13ΔAA; lane 6, mutant V13A+B; lane 7, mutant V13Δ97. **C,D:** Lane 1, wild-type pJV16; lane 2, YJV100 cells carrying a plasmid without an rDNA unit; lanes 3 and 4, mutant V3Δ93; lanes 5 and 6, mutant V3Δ181.

parently, in these mutants, processing at A3 is not followed by exonucleolytic trimming to $B1_S$. Instead, the $27S_{A3}$ pre-rRNA appears to be cleaved at a site downstream from probe 2B, but upstream from the tag in 25S rRNA. Because no aberrant stop was detectable in primer extension analysis using the oligonucleotide complementary to the 25S tag (data not shown), we conclude that this cleavage takes place at site C1. Thus, we conclude that, in the V3Δ93 and V13Δ181 mutants, the $B1_L$ processing pathway operates normally, although at a reduced rate. The sequence of processing events in the $B1_S$ route, however, seems to be altered in such a way that cleavage at C1 now precedes processing at $B1_S$. This altered processing route should, in principle, give rise to a fragment extending from A3 to C1, but we were unable to detect such a fragment by means of northern hybridization (which is less sensitive than primer extension analysis) using probe 2A. This indicates that it must be processed rapidly at sites $B1_S$ and C2 in that order, because $B1_S$ is detected with primer 2B, located downstream from site C2 (Fig. 8), and $7S_S$ pre-rRNA is visible in a northern hybridization using probe 2A (Fig. 6D). Alternatively, the A3–C1 fragment might be subject to 3′ → 5′ exonucleolytic degradation.

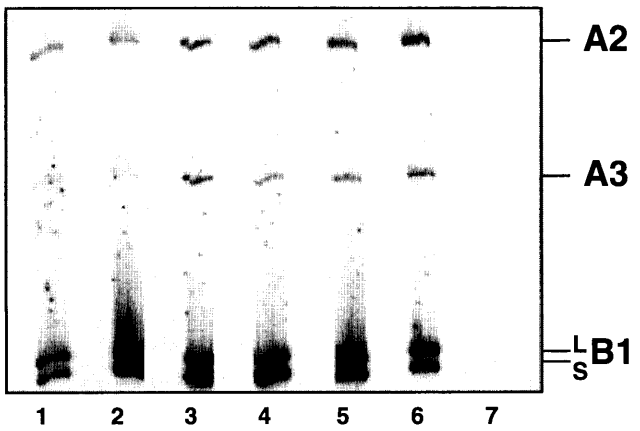

FIGURE 7. Primer extension analysis of RNA from V13 mutants. Total RNA was extracted from YJV100 transformants 16 h after transfer to YNB-glucose and analyzed by primer extension using the probe 2B (cf. Fig. 4). Processing sites corresponding to the primer extension stops are indicated on the right. Lanes 1 and 6, wild-type pJV12; lane 2, mutant V13Δ111; lane 3, mutant V13Δ131; lane 4, mutant V13ΔAA; lane 5, mutant V13A+B; lane 7, YJV100 cells carrying a plasmid without an rDNA unit.

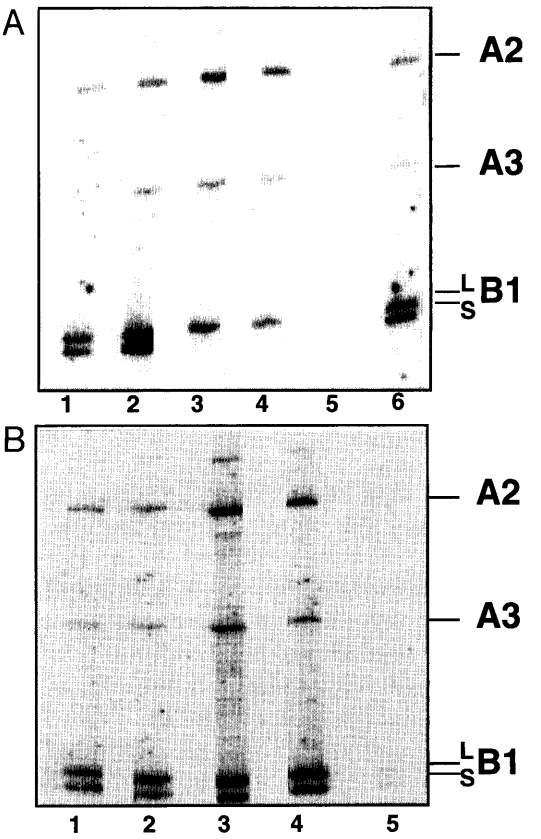

FIGURE 8. Primer extension analysis of RNA from V3 mutants. Total RNA was extracted from YJV100 transformants 16 h after transfer to YNB-glucose and analyzed by primer extension. Processing sites corresponding to the primer extension stops are indicated on the right. **A:** Primer extension analysis from within the mature 25S rRNA sequence using the oligonucleotide complementary to the tag. Lanes 1 and 6, wild-type pJV12; lane 2, mutant V3Δ44; lane 3, mutant V3Δ93; lane 4, mutant V3Δ181; lane 5, YJV100 cells carrying a plasmid without an rDNA unit. **B:** Primer extension analysis from within ITS2 using probe 2B (cf. Fig. 4). Lane 1, wild-type pJV12; lane 2, mutant V3Δ44; lane 3, mutant V3Δ93; lane 4, mutant V3Δ181; lane 5, YJV100 cells carrying a plasmid without an rDNA unit.

DISCUSSION

In this paper, we report the in vivo effect of a series of deletion and point mutations (Figs. 1, 2) in variable regions V13 and V3 of *S. cerevisiae* 25S rRNA. The phenotypes caused by these mutations were analyzed using the "in vivo Pol II" system in which yeast cells can be made completely dependent on mutant, plasmid-encoded rRNA. Removal of distinct structural elements by a series of progressively larger deletions of V13 demonstrated that helix E20_1 is completely dispensable for 60S subunit biogenesis or ribosome function. Mutant V13Δ97 containing this deletion does not show any growth defect (Fig. 2A) and produces normal amounts of mature 18S and 25S rRNA, as well as $27S_A$ and $27S_B$ pre-rRNA (data not shown). These results indicate that the lethal phenotype caused by inserting 119 nt into helix 20_1 of *T. thermophila* V13 (Sweeney et al., 1994) is not due to destruction of an essential functional element, but rather to disturbance of the folding of the (pre-)rRNA or steric hindrance of its assembly with ribosomal proteins. Reducing V13 to the approximate size of its prokaryotic counterpart (mutant V13Δ131) proved to be lethal (Fig. 2D), which corroborates previous observations with respect to the functional importance of V13 in *T. thermophila* (Sweeney et al., 1994). The essential structural elements are limited to helix E20 because mutation V13Δ111 lacking both E20_1 and E20_2 is still able to support growth, albeit relatively poorly (Fig. 2B). Mutation V13Δ97C, on the other hand, does not affect the growth rate, demonstrating that the primary structure of the E20_2 helix is irrelevant (Fig. 2C). This is in agreement with the functional equivalence observed in vivo for the *T. thermophila*, *S. cerevisiae*, *Dictyostelium discoideum*, and *Caenorhabditis elegans* V13 regions (Sweeney et al., 1994) despite considerable sequence differences between their respective E20_2 helices. The latter observation also suggests that the size of helix E20_2, which ranges from 3 bp in *T. thermophila* and *D. discoideum* to 7 bp in *C. elegans*, is not critical.

Helix E20 appears to contain at least two distinct essential structural elements. A deletion that includes its upper portion (mutation V13Δ131) is lethal, as are the point mutations V13A+B and V13ΔAA in its lower portion. We conclude that the essential features within these two regions of V13 are most likely secondary structural, rather than specific sequence, elements. As far as the upper portion of helix E20 is concerned, this is again supported by the limited sequence similarity in this region between the E20 helices of the functionally equivalent *T. thermophila*, *D. discoideum*, *S. cerevisiae*, and *C. elegans* V13 regions (Schnare et al., 1996). With respect to the lower portion, the neutral character of the V13A and V13B mutations (Fig. 2E,F) shows that the sequence alterations per se are not the cause of the lethal phenotype of the V13A+B mutation. The lethal effect of removing the two bulged A residues (mutation V13ΔAA; Fig. 2H) further supports the importance of secondary, rather than primary, structure. Clearly, an interruption of the normal base pairing is an essential feature of this region of V13. However, even though this interruption always consists of a 2-nt bulge at the 3′ side, in many cases containing two A residues (Schnare et al., 1996), the number, distribution, and precise identity of the unpaired nucleotides does not appear to be critical, as shown by the neutral character of the V13A and V13B mutations (Fig. 2) and the fact that *C. elegans* V13 contains a GU bulge at this position. In other organisms, unpaired GG, GA, or AG sequences are present (Gutell et al., 1993). On the other hand, the lethality of the V13A+B mutation demonstrates that not just any base pairing irregularity will suffice. Sweeney et al. (1994) have made similar observations in their mutational analysis of *T. thermophila* V13. The precise requirements for this region of V13, however, can only be revealed by detailed structural analysis.

Analysis of pre-rRNA processing in the lethal V13Δ131, V13A+B, and V13ΔAA mutants showed a substantial accumulation of the $27S_B$ precursor species, whereas mature 25S and 5.8S rRNA were (almost) completely absent (Figs. 3, 5). Apparently, these mutations strongly reduce the efficiency of ITS2 processing. However, 7S pre-rRNA remains detectable (Fig. 6), which demonstrates that ITS2 processing does not come to a complete standstill. We therefore assume that the 5.8S/25S rRNA resulting from this residual processing is degraded rapidly, probably because it is part of a structurally imperfect subunit.

Such structural imperfection might be the result of failure of the (pre-)rRNA to be (correctly) recognized by ribosomal proteins. Assembly defects can indeed cause instability of rRNA as well as perturb processing (Underwood & Fried, 1990; Moritz et al., 1991). Although there is no direct evidence for an r-protein binding site within V13, we note that the presence of structural irregularities, such as bulged nucleotides, in RNA helices is important in many ribosomal protein–rRNA interactions (e.g., Peattie et al., 1981; Wu & Uhlenbeck, 1987; Gregory et al., 1988).

Deletion analysis of the V3 variable region of yeast 25S rRNA demonstrated that partial removal of the outer C1_2 helix of this region (mutant V3Δ44) caused a severe growth defect, whereas amputation of the complete helix (mutant V3Δ93) was lethal (Fig. 2I,J). Interestingly, the latter mutant appears to be defective in the removal of the ITS1 fragment from the $27S_A$ pre-rRNA. As demonstrated by northern analysis (Fig. 5), the V3Δ93 mutation, and also the larger V3Δ181 mutation, caused a substantial increase in the level of the $27S_A$ precursor species, indicating that its conversion into $27S_B$ pre-rRNA is delayed. Because we could

detect stops corresponding to the A3 and $B1_L$ cleavage sites by primer extension from within the mature 25S rRNA sequence (Fig. 8A), we conclude that the $27S_{A2} \rightarrow 27S_{A3}$ and $27S_{A2} \rightarrow 27S_{BL}$ processing steps are performed correctly, although possibly with reduced efficiency, in the two V3 deletion mutants. In contrast, the pathway leading from the $27S_{A3}$ precursor to 5.8S/25S rRNA, which under normal conditions is the major route for production of the mature LSU rRNA species (Henry et al., 1994; cf. Fig. 4B), is seriously disturbed. The complete absence of a stop corresponding to $B1_S$ upon primer extension from within mature 25S rRNA (Fig. 8A, lanes 3 and 4) clearly indicates that $27S_{A3}$ pre-rRNA fails to be converted into $27S_{BS}$. This is not due to a lack of ability of the processing machinery to remove the A3–$B1_S$ fragment because primer extension using probe 2B produced a clear stop corresponding to $B1_S$ (Fig. 8B, lanes 3 and 4). Because probe 2B is complementary to the region of ITS2 between sites C2 and C1 (cf. Fig. 4A) and primer extension from within 25S rRNA did not reveal any stops upstream from C1, the mature 5′ end of 25S rRNA, we interpret these observations as follows. In the V13Δ93 and V13Δ181 mutants, significant processing of $27S_{A3}$ pre-rRNA still occurs. However, this processing proceeds via initial cleavage at site C1. The aberrant A3–C1 fragment must then be processed rapidly at sites $B1_S$ and C2 because the $7S_S$ pre-rRNA is clearly detectable (Fig. 6D). Processing at site E may occur, but any resulting mature 5.8S rRNA/25S rRNA produced by this aberrant, or by the normal $B1_L$, pathway is highly unstable.

That an intact V3 region is important for normal, stable accumulation of mature 5.8S/25S rRNA is further supported by the phenotype of the V3Δ44 mutation. In contrast to the larger deletions, this mutation had no detectable effect on pre-rRNA processing but, nevertheless, reduced the level of 25S rRNA about twofold (Fig. 3). This indicates that removal of the tip of the C1_2 helix affects turnover, rather than production, of these rRNA species. Interestingly, Sweeney et al. (1996) recently reported that insertions into the C1_2 helix of *Tetrahymena* 26S rRNA at a position corresponding to the arrow in Figure 1 (i.e., just before the start of the Δ44 deletion) did not have any deleterious effect, indicating a high degree of structural flexibility in this region of V3. This structural flexibility is also evident from the extreme variation in size of V3, which ranges from 8 nt in *Giardia* species to 865 nt in humans (Schnare et al., 1996).

In conclusion, the results reported in this paper clearly demonstrate that both the V13 and V3 variable regions of *S. cerevisiae* 25S rRNA contain elements that are important, or even essential, for normal biogenesis and stability of the LSU rRNAs, and begin to identify the location and nature of these elements in more detail.

MATERIALS AND METHODS

Strains

The *E. coli* strains Sure™ Strain (Stratagene, La Jolla, California), JM109, and BMH 71-18 *mutS* were used as bacterial hosts and used for cloning experiments. *S. cerevisiae* strain YJV100 [*Matα, rpa135::LEU2, ade2-1, his3-11, leu2-3,112, trp1-1, ura3-1, can1-100, RDN1::pGRIM (TRP1d, GAL7-rDNA)*; Venema et al., 1995a] is defective in RNA polymerase I. This strain is rescued by multiple integrated copies of an rDNA unit under control of an inducible *GAL7* promoter. Growth and handling of *S. cerevisiae* and *E. coli* were performed by standard techniques.

Plasmids

The plasmid pJV12 (*2μ, URA3*) is a YEplac 195 (Gietz & Sugino, 1988) derivative and contains an rDNA unit under control of the *PGK1* promoter. The rDNA unit contains small oligonucleotide tags in the 18S rRNA (Beltrame et al., 1994) and the 25S rRNA (Musters et al., 1989b). The plasmid pJV16, which contains a third tag located in the 5.8S rRNA sequence, was constructed by exchanging a 1.5-kb *Sac* I–*Xho* I fragment, including the 5.8S rRNA sequence (cf. Fig. 4), for a *Sac* I–*Xho* I fragment from the pGAL::rDNA plasmid carrying the 5.8S rRNA tag (Henry et al., 1994). The plasmid pGEM3-SacMlu4 was constructed by cloning a 2-kb *Sac* I–*Mlu* I fragment from pJV12, extending from 18S rRNA into 25S rRNA (cf. Fig. 4), into pGEM3 (Promega, Madison, Wisconsin) with the use of a *Mlu* I–*Sma* I linker. The plasmid pGEM3ΔN-25SSacSal was obtained by cloning a 4.0-kb *Sac* I–*Sal* I rDNA fragment (cf. Fig. 3) into pGEM3, in which the *Nar* I sites present in the vector had been destroyed previously.

Site-directed mutagenesis

The vector pAlter-SacMlu4 is a derivative of pAlter1 (Promega) and contains the same 2.0-kb *Sac* I–*Mlu* I rDNA fragment as pGEM3-SacMlu4 (see above). The plasmid pAlter-25SXH3 contains a 2.5-kb *Xba* I–*Hind* III 25S rRNA fragment obtained from pJV12 and cloned into pAlter1. Using the pAlter derivatives as templates, mutations were introduced into V3 (pAlter-SacMlu4) and V13 (pAlter-25SXH3) by the Altered Sites® II in vitro mutagenesis system (Promega) according to the supplier's instructions. The presence of the mutations was verified by DNA sequencing (Sequenase® 2.0 kit, USB, Cleveland, Ohio). Mutations in variable region V3 were transferred to pJV12 by exchanging its 0.6-kb *Xho* I–*Mlu* I fragment for the mutated fragment. The mutations V3Δ93 and V3Δ181 were cloned in the pJV16 plasmid by exchanging the *Sph* I–*Mlu* I fragment from pJV16 for the corresponding fragment carrying the mutation. V13 mutations were first subcloned into pGEM3ΔN-25SSacSal (see above) by exchanging the wild-type *Bgl* II–*Nar* I rDNA fragment for the mutated fragment and subsequently cloned as a 3-kb *Mlu* I–*Sal* I fragment (cf. Fig. 4A) into pJV12. The V13Δ97C mutation was obtained by inserting a linker into the *Sac* I site of the pGEM3ΔN-25SSacSal-V13Δ111 mutation and subsequently cloned into pJV12. The pJV16 derivatives pJV16-V13Δ97, pJV16-V13Δ111, pJV16-V13Δ131, and pJV16-V13ΔAA were constructed by replacing the wild-type *Mlu* I-

Sal I fragment of pJV16 with the mutated fragment from the pertinent pJV12 derivative. The V3 and V13 mutations described in this study and their putative secondary structures are depicted in Figure 1.

Determination of growth rate

YJV100 cells were transformed with the pJV12 derivative carrying the desired mutation and transformants were grown in liquid YNB medium containing 2% (w/v) galactose at 30 °C until mid-log phase was reached (OD_{660} ~0.8). An aliquot of the culture was centrifuged (3 min, 700 g, 30 °C), resuspended in pre-warmed YNB medium containing 2% (w/v) glucose to give an OD_{660} of 0.05, and further incubated at 30 °C. The OD_{660} of the culture was then measured at regular intervals over a period of several doubling times. Cultures were diluted regularly to maintain exponential growth. Cells were checked routinely for morphological abnormalities by phase-contrast microscopy and found to be normal in all cases.

Northern and primer extension analysis of (pre-)rRNA

Yeast cells were shifted to YNB-glucose as described above and incubated for 16 h at 30 °C. Total RNA was isolated as described previously (Musters et al., 1989a, 1990). For northern analysis, 5 μg of RNA was separated on either a 1.2% or 2% agarose/formaldehyde gel according to Venema et al. (1995b), blotted, and hybridized to different oligonucleotide probes. For detection of short processing products, an 8% polyacrylamide gel was used according to Venema et al. (1995b). Hybridization signals were visualized using a phosphorimager and RNA levels were quantified using the programme ImageQuant (Molecular Dynamics, Sunnyvale, California). Primer extension analysis was performed as described by Beltrame and Tollervey (1992) using 0.4 μg of RNA. Locations of the probes used for detection of the various (pre-)rRNA species and for primer extension are depicted in Figure 4.

ACKNOWLEDGMENTS

We thank Jan Boesten for synthesizing the deoxyoligonucleotides used in these experiments. J.V. is a fellow of the Royal Netherlands Academy of Sciences. This work was supported by a Human Frontier Science Program grant (#RG-360/93) to H.A.R.

Received January 2, 1997; returned for revision January 25, 1997; revised manuscript received February 5, 1997

REFERENCES

Beltrame M, Henry Y, Tollervey D. 1994. Mutational analysis of an essential binding site for the U3 snoRNA in the 5′ external transcribed spacer of yeast pre-rRNA. *Nucleic Acids Res 22*:5139–5147.

Beltrame M, Tollervey D. 1992. Identification and functional analysis of two U3 binding sites on yeast preribosomal RNA. *Embo J 11*:1531–1542.

De Rijk P, Van der Peer Y, De Wachter R. 1996. Database on the structure of large ribosomal subunit RNA. *Nucleic Acids Res 24*:92–97.

Gerbi SA. 1996. Expansion segments: Regions of variable size that interrupt the universal core secondary structure of ribosomal RNA. In: Zimmermann RA, Dahlberg AE, eds. *Ribosomal RNA: Structure, evolution, processing and function in protein biosynthesis*. Boca Raton, Florida: CRC Press. pp 71–87.

Gietz RD, Sugino A. 1988. New yeast-*Escherichia coli* shuttle vectors constructed with in vitro mutagenized yeast genes lacking six-base pair restriction sites. *Gene 74*:527–534.

Gregory RJ, Cahill PBF, Thurlow DL, Zimmermann RA. 1988. Interaction of *Escherichia coli* ribosomal protein S8 with its binding sites in ribosomal RNA and messenger RNA. *J Mol Biol 204*:295–307.

Gutell RR, Gray MW, Schnare MN. 1993. A compilation of large subunit (23S and 23S-like) ribosomal RNA structures. *Nucleic Acids Res 21*:3055–3077.

Henry Y, Wood H, Morrissey JP, Petfalski E, Kearsey S, Tollervey D. 1994. The 5′ end of yeast 5.8S rRNA is generated by exonucleases from an upstream cleavage site. *EMBO J 13*:2452–2463.

Kooi EA. 1995. The role and nature of the interaction between ribosomal protein L25 and 26S rRNA in yeast ribosomes [thesis]. Amsterdam: Vrije Universiteit.

Moritz M, Pulaski BA, Woolford JL Jr. 1991. Assembly of 60S ribosomal subunits is perturbed in temperature-sensitive yeast mutants defective in ribosomal protein L16. *Mol Cell Biol 11*:5681–5692.

Musters W, Boon K, Van der Sande CAFM, Van Heerikhuizen H, Planta RJ. 1990. Functional analysis of transcribed spacers of yeast ribosomal DNA. *EMBO J 9*:3989–3996.

Musters W, Gonçalves PM, Boon K, Raué HA, Van Heerikhuizen H, Planta RJ. 1991. The conserved GTPase center and variable region V9 from *Saccharomyces cerevisiae* 26S rRNA can be replaced by their equivalents from other prokaryotes and eukaryotes without detectable loss of ribosomal function. *Proc Natl Acad Sci USA 88*:1469–1473.

Musters W, Knol J, Maas AF, Dekker H, Van Heerikhuizen H, Planta, RJ. 1989a. Linker scanning of the yeast RNA polymerase I promoter. *Nucleic Acids Res 17*:9661–9678.

Musters W, Venema J, Van der Linden G, Van Heerikhuizen H, Klootwijk J, Planta RJ. 1989b. A system for the analysis of yeast ribosomal DNA mutations. *Mol Cell Biol 9*:551–559.

Nogi Y, Yano R, Nomura M. 1991. Synthesis of large rRNAs by RNA polymerase II in mutants of *Saccharomyces cerevisiae* defective in RNA polymerase I. *Proc Natl Acad Sci USA 88*:3962–3966.

Noller HF. 1991. Ribosomal RNA and translation. *Annu Rev Biochem 60*:191–227.

Noller HF, Green R, Heilek G, Hoffarth V, Hüttenhofer A, Joseph S, Lee I, Lieberman K, Mankin A, Merryman C, Powers T, Puglisi EV, Samaha RR, Weiser B. 1995. Structure and function of ribosomal RNA. *Biochem Cell Biol 73*:997–1009.

Noller HF, Hoffarth V, Zimniak L. 1992. Unusual resistance of peptidyl transferase to protein extraction procedures. *Science 256*:1416–1419.

O'Connor M, Brunelli CA, Firpo MA, Gregory ST, Lieberman KR, Lodmell JS, Moine H, Van Ryk DI, Dahlberg AE. 1995. Genetic probes of ribosomal RNA function. *Biochem Cell Biol 73*:859–868.

Peattie DA, Douthwaite S, Garrett RA, Noller HF. 1981. A "bulged" double helix in a RNA-protein contact site. *Proc Natl Acad Sci USA 78*:7331–7335.

Raué HA, Klootwijk J, Musters W. 1988. Evolutionary conservation of structure and function of high molecular weight rRNA. *Prog Biophys Mol Biol 51*:77–129.

Raué HA, Planta RJ. 1995. The pathway to maturity: Processing of ribosomal RNA in *Saccharomyces cerevisiae*. *Gene Expr 5*:71–77.

Schnare M, Damberger SH, Gray MW, Gutell RR. 1996. Comprehensive comparison of structural characteristics in eukaryotic cytoplasmic large subunit (23 S-like) ribosomal RNA. *J Mol Biol 256*:701–719.

Sweeney R, Chen L, Yao MC. 1993. Phenotypic effects of targeted mutations in the small subunit rRNA gene of *Tetrahymena thermophila*. *Mol Cell Biol 13*:4814–4825.

Sweeney R, Chen L, Yao MC. 1994. An rRNA variable region has an evolutionarily conserved essential role despite sequence divergence. *Mol Cell Biol 14*:4203–4215.

Sweeney R, Fan Q, Yao MC. 1996. Antisense ribosomes, rRNA as a vehicle for antisense RNAs. *Proc Natl Acad Sci USA 93*:8518–8523.

Sweeney R, Yao MC. 1989. Identifying functional regions of rRNA by insertion mutagenesis and complete gene replacement in *Tetrahymena thermophila*. *EMBO J 8*:933–938.

Triman KL. 1996a. The 16S ribosomal RNA mutation database (16SMDB). *Nucleic Acids Res 24*:166–168.

Triman KL. 1996b. The 23S ribosomal RNA mutation database (23SMDB). *Nucleic Acids Res 24*:169–171.

Underwood MR, Fried HM. 1990. Characterization of nuclear localizing sequences derived from yeast ribosomal protein L29. *EMBO J 9*:91–99.

Van der Peer Y, Nicolaï S, De Rijk P, De Wachter R. 1996. Database on the structure of small ribosomal subunit RNA. *Nucleic Acids Res 24*:86–91.

Van Nues RW, Rientjes JMJ, Morré SA, Mollee E, Planta RJ, Venema J, Raué HA. 1995. Evolutionary conserved structural elements are critical for processing of Internal Transcribed Spacer 2 from *Saccharomyces cerevisiae*. *J Mol Biol 250*:24–36.

Van Nues RW, Venema J, Planta RJ, Raué HA. 1993. Ribosomal RNA processing in *Saccharomyces cerevisiae*. In: Nierhaus KH, Subramanian AR, Erdmann VA, Franceschi F, Wittmann-Liebold B, eds. *The translational apparatus*. New York: Plenum Press. pp 151–162.

Van Nues RW, Venema J, Planta RJ, Raué HA. 1997. Variable region V1 of *Saccharomyces cerevisiae* 18S rRNA participates in biogenesis and function of the small ribosomal subunit. *Chromosoma*. Forthcoming.

Venema J, Dirks-Mulder A, Faber AW, Raué HA. 1995a. Development and application of an in vivo system to study yeast ribosomal RNA biogenesis and function. *Yeast 11*:145–156.

Venema J, Henry Y, Tollervey D. 1995b. Two distinct recognition signals define the site of endonucleolytic cleavage at the 5′-end of yeast 18S rRNA. *EMBO J 14*:4883–4892.

Venema J, Tollervey D. 1995. Processing of pre-ribosomal RNA in *Saccharomyces cerevisiae*. *Yeast 11*:1629–1650.

Wu HN, Uhlenbeck OC. 1987. Role of a bulged A residue in a specific RNA-protein interaction. *Biochemistry 26*:8221–8227.